Exp Brain Res (1991) 84:195–209

Experimental Brain Research

A quantitative analysis of cytochrome oxidase-rich patches in the primary visual cortex of *Cebus* monkeys: topographic distribution and effects of late monocular enucleation

M.G.P. Rosa, R. Gattass, and J.G.M. Soares

Departamento de Neurobiologia, Instituto de Biofísica Carlos Chagas Filho, Universidade Federal do Rio de Janeiro, Cidade Universitária – CCS – Bloco G, Ilha do Fundão, Rio de Janeiro 21941, Brazil

Received May 8, 1990 / Accepted September 28, 1990

Summary. We have studied the tangential distribution of cytochrome oxidase (cytox)-rich patches in striate cortex of normal and monocularly enucleated *Cebus apella* monkeys. Patch spatial density and patch cross-sectional area were analysed in cytox-reacted tangential sections of flat-mounted preparations of V1. In the upper cortical layers of V1, and specially in the middle of layer III, the *Cebus* has well-delimited cytox-rich patches. Rows of patches are less conspicuous in *Cebus* than in Old World monkeys. The spatial density of patches is nearly constant throughout the binocular field representation in V1, with a mean value of 4 patches per mm^2. In the monocular portions of V1, however, patch spatial density diminishes. In most cases, mean patch cross-sectional area decreases slightly towards the representation of the periphery in V1. However, patches in the representation of the monocular crescent tend to be larger than those in the adjacent binocular representation. The small variation of cytox patch topography with eccentricity contrasts with the large variation of cortical point-image size in V1. In monocularly enucleated monkeys, patches are larger and darker above and below the ocular dominance stripes of the remaining eye than in the alternate stripes. After long-term enucleation, the patches corresponding to the remaining eye columns appeared larger than in normal controls. In contrast, there is no difference in size between the patches located in the deprived and undeprived monocular crescent representations, although both patch and interpatch regions are darker staining in the latter. These results suggest the existence of competitive interactions which modify the cortical intrinsic organization even in adult monkeys.

Key words: Striate cortex – Modular organization – Plasticity – Platyrrhini – Ocular dominance – Monkey

Offprint requests to: M.G.P. Rosa (address see above)

Introduction

Current ideas on the nature of the processing of visual information in the cortex of mammals are largely basen on the concept of cortical modules. The idea of repetitive subunits which analyse visual attributes of the image in small portions of the visual field was derived from single-unit studies by Hubel and Wiesel (for a review, see Hubel and Wiesel 1977) in the striate cortex (V1) of monkeys. These authors demonstrated that the size of the cortical region in V1 which represents a given point of the visual field would be about 2 mm at the region of representation of the central 20° of the visual field. The linear dimension of the cortical "point image" (Mc Illwain 1976) decreases towards peripheral V1 (Dow et al. 1981) but is always large enough to contain neurons selective to all orientations and with dominance for each eye. The modular theory was strongly supported by the discovery of a periodic arrangement of functionally distinct subregions in primate V1, demonstrated by cytochrome oxidase (cytox) histochemistry (Horton and Hubel 1981; Livingstone and Hubel 1984). The cytox-rich "blobs" (Livingstone and Hubel 1984) or "patches" (Horton 1984) maintain invariant topographic relationships with ocular dominance (Horton and Hubel 1981) and orientation (Blasdel and Salama 1986) columns. These patches can, therefore, be used as anatomical markers of a cortical modular organization.

Cebus apella, the tufted capuchin monkey, is a species currently used as a model of New World monkey for studies of the visual system (Gattass et al. 1978, 1987, 1990a, b; Hess and Edwards 1987; Rosa et al. 1988b, c; Fiorani et al. 1989; Silveira et al. 1989). The *Cebus* is well suited for comparisons with Old World monkeys in view of its diurnal habits, as well as its size and brain sulcal pattern, which are similar to those of *Macaca fascicularis* (Le Gros Clark 1959; Freese and Oppenheimer 1981). In

a study of ocular dominance stripes in the New World monkey *Cebus*, we found that the width of a pair of stripes varied only slightly with eccentricity for most of V1 (Rosa et al. 1988b). As cytox patches occupy a central position relative to these stripes (Hess and Edwards 1987), this observation suggests that the topographic distribution of patches is invariant in V1 of *Cebus*. In this respect, the *Cebus* would be different from *Macaca*, since in the latter species the number of patches per square millimeter increases with increasing eccentricity (Horton 1984; Livingstone and Hubel 1984). In contrast, the visual topography, the magnification factors and the orientation of ocular dominance stripes in V1 are similar in these genera (Gattass et al. 1987; Rosa et al. 1988b). Here, we describe the anatomical distribution of cytox patches in different portions of V1 in *Cebus apella* monkeys, as well as the effects of monocular enucleation on patch topography. Preliminary accounts of these data were published elsewhere (Rosa et al. 1988a; Gattass et al. 1990a).

Material and methods

Five cerebral hemispheres from two male (CO4, CO10) and one female (CO7) adult *Cebus apella* monkeys were used. Ophthalmoscopic inspection of the eye fundus insured that all animals were free from gross retinal abnormalities. In addition, we also examined striate cortices from three other adult monkeys, which were monocularly enucleated for 18 days (CO11), 4 months (CO6) and 7 months (CO5). In these monkeys, monocular enucleation was performed under Saffan (Glaxovet, Alphaxalone 10 mg/kg and Alphadolone 3 mg/kg) and Ketalar (Parke-Davis, Ketamine HCl 30 mg/kg) anesthesia and aseptic conditions. A quantitative analysis of the cytox patches was performed in sections nearly tangential to cortical layer III, from flattened preparations of striate cortex and adjoining areas. Striate cortices from two other normal monkeys (CO1 and CO2) were not fully analysed in a quantitative manner, but were used to confirm the data regarding laminar distribution and regional differences of cytox patterns in V1.

In order to obtain flat-mounts of V1, monkeys were deeply anesthetized with ketamine HCl (50 mg/kg), followed by a lethal dose os sodium pentobarbital. Right after the occurrence of pharmacological apnea the monkeys were intracardially perfused with a 10% sucrose in phosphate buffer 0.1 M, pH 7.4 solution. Subsequently, the posterior portion of the brains underwent the flat-mounting procedure described by Tootell and Silverman (1985, method II). The flat-mounted blocks were fixated between parafilm-covered glass slides either in a 2.5% glutaraldehyde/10% sucrose in phosphate buffer solution for 48 h (most cases) or in 4% formaldehyde for 24 h (CO4R). After fixation, the blocks were quickly frozen and cut at 40 μm in a cryostat. The sections were immediately mounted in gelatinized slides, dried on a hot plate and stored overnight in phosphate buffer. Cytochrome oxidase histochemical reaction followed the procedure modified by Silverman and Tootell (1987) from the protocol of Wong-Riley (1979). Stained sections were dehydrated, defatted and coverslipped. Case CO11, the 18-day enucleated animal (also used for other studies), was perfused with 2% paraformaldehyde/1% glutaraldehyde in buffered sucrose, and had its hemispheres sectioned in standard parasagittal and coronal planes. Otherwise, histological procedures were similar.

The sections were photographed using Kodak Plus-X film under blue light illumination to increase contrast. Reconstruction of the pattern of cytox patches was accomplished by superimposing photographs of serial sections, using blood vessels as landmarks (Rosa et al. 1988b; see also Fig. 3). For quantitative analysis, patches were outlined with finepoint permanent marker on enlarged (21 X), contrast-matched prints of each section. The outlined patches were then measured on a graphic tablet interfaced to an Apple II computer. In outlining patch boundaries, it was found useful to use slightly defocused photographs (see Fig. 1), in order to cut high spatial frequency components of the image; this procedure was specially useful in analysing regions where patches appeared in low contrast.

As shows in *Results* (Fig. 2), estimates of the borders of a given patch may vary depending on the cortical layer analysed. We therefore chose to analyse patch topography at the middle portion of layer III, which shows the highest contrast between cytox-rich and cytox-poor tissue. Bias introduced by different experimenters was negligible. There was no statistical difference ($P > 0.3$, *t*-test) in measurements performed in the same hemisphere by different subjects. Nonetheless, for any given case, the measurements presented here have always been performed by one observer. As an additional control, in some sections we performed optical scans (Fig. 1) with the aid of a Logitech hand scanner. The hand-drawn and the computer-generated maps of patches show a fairly good agreement (Fig. 1). Therefore, the fuzziness of patch boundaries at peripheral V1 does not seem to invalidate the analysis of patch sizes. Figure 1 illustrates the definition of patch borders in photographs by hand outlines and computer scans, with the same magnification used for the quantitative analysis.

In each hemisphere, some cortical regions were not analyzed, due to tissue injury during the flattening procedure, to histological artifacts or to the existence of tissue distortion greater than 5%. Distortion in the sections was evaluated by inserting, prior to the flattening procedure, several triplets of marking pins at known distances, perpendicular to the surface of the brain with the sulci gently opened. The comparison of the original distance with the distance measured in the sections was done in three different orientations parallel to the cortical surface, in 10 different locations in each hemisphere. Linear distortion, as evaluated by this method, did not exceed 5% for most of V1. However, regions of greater distortion were observed at specific portions of V1 in different monkeys. These regions were located mainly at the vicinity of the fundi of sulci, as well as along the posterior convexity of the brain. As an additional measure, in three hemispheres we introduced discontinuities in V1 to minimize the effect of distortions. In one of these hemispheres (CO10L) we were unable to observe any distortion, as evaluated by the reference pins.

The assignment of retinotopic coordinates to specific sites in flat-mounted V1 was made based on the study of Gattass et al. (1987). We have employed the integration of the isopolar cortical magnification factor (Mp) of V1, expressed by equation (1), to locate the isoeccentricity lines in the maps.

$$\text{Ln (Mp)} = 1.63 - 0.39 \text{ Ln (ecc)} - 0.11 \text{ Ln (ecc)}^2 \quad (1)$$

Although similar to equation (6) from Gattass et al. (1987), equation (1) was chosen because it was based on the mean Mp of V1 from the original case of Gattass et al. (1987) and two additional extensively studied monkeys. In view of the variability in size of V1 observed among different monkeys, we have multiplied the values of Mp by constants to match the measured extent of the horizontal meridian representation (i.e., the longer axis of the flatmounted V1) to that predicted by the Mp function.

Results

In *Cebus*, as in most primates (Horton 1984), the cytox patches are more conspicuous in the supragranular layers, specially in layer III (Fig. 2). They are also visible in layer IVb and in the infragranular layers, although with less contrast (Fig. 2). Our results confirm the laminar distribution of cytox patches in V1 of *Cebus* monkeys, as described in detail by Hess and Edwards (1987). The

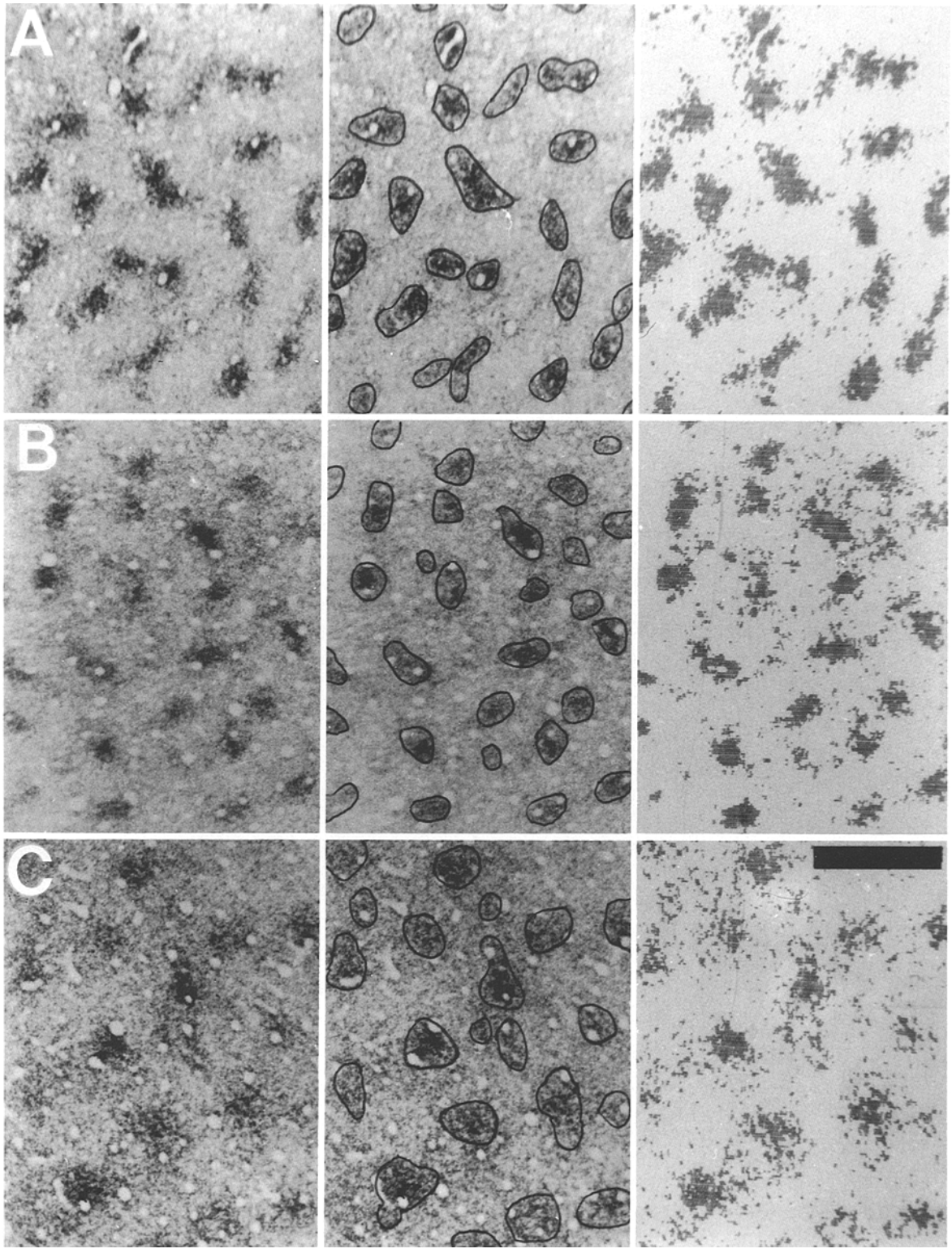

Fig. 1A–C. Criteria used to draw cytox patch borders. *Left:* photographs of cytox patches in V1 of case CO4L, shown at the same magnification used for data analysis; *middle:* same regions, after outlining the patches: *right:* computer-generated optical scans of the same regions. Row A corresponds to patches at 3°, row B at 40° and row C at monocular crescent V1. Scale bar = 1 mm

quantitative analysis presented here concentrates on the size and distribution of patches at middle third of layer III, where they are better delineated throughout V1.

In Fig. 3, portions of adjacent sections through layer III of V1 were combined in order to reconstruct the pattern of patches for case CO4L. As in other species of monkeys (Horton 1984), cytox patches in *Cebus* tend to be oval is shape. In some regions, adjacent patches are linked by bridges of cytox-reactive tissue, forming rows. In *Cebus* the patches tend to be more individualized than

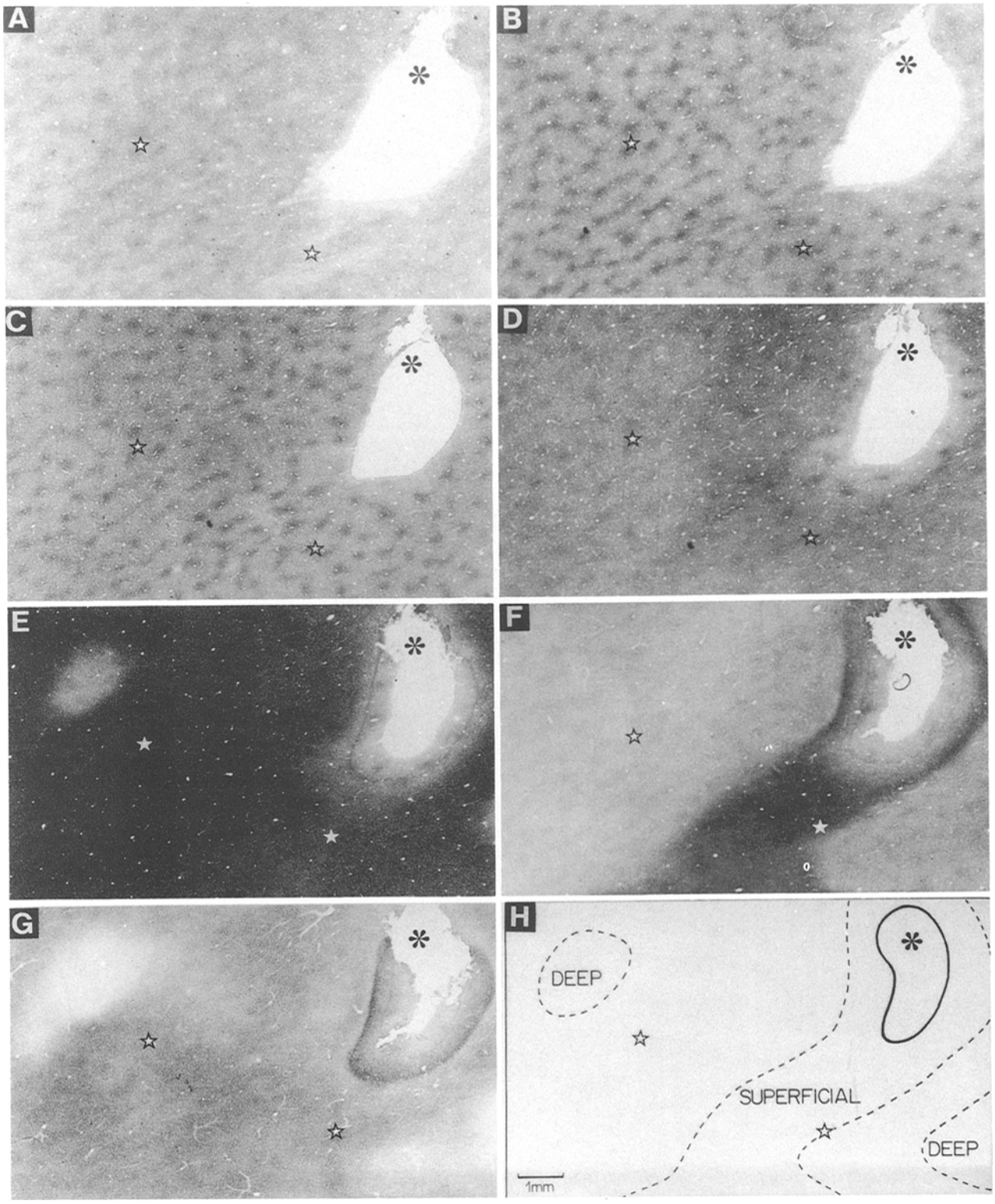

Fig. 2A–H. Series of cytox-stained tangential sections through the representation of central lower quadrant, showing the variation in the appearance of patches across cortical layers. In all sections, a similar pair of blood vessels is labelled with *stars*, and a hole artifact with *asterisks*. The plane of section is not exactly parallel to the cortical layers, as shown in insert **H**. Therefore, these sections reveal both laminar and tangential features of cytox topography in V1. **A** A superficial section, through layer II. Cytox patches are faintly seen in the left portion of this figure, but cannot be seen in the more superficial regions. **B** A section mostly through the middle of layer III, where patches are darkest. The more superficial regions show well-defined, albeit lighter patches. **C** In the lower third of layer III, patches are small, light and show less defined borders, while in more superficial regions they are dark and well-defined. **D** In layer IVb *(left)*, the overall staining in the interpatch region is increased as compared with layers II and III, and cytox patches can be faintly distinguished. This section also grazes through layer IVa, the dark region immediately left to the portion of layer III surrounding the hole. **E** Deep in layer IVc, staining is overall intense, and patches cannot be seen. The region surrounding the hole shows a sequence including layer III *(inner)*, IVa, IVb and superficial IVc. A small piece of layer V *(light tissue)* is shown at the *upper left*. **F** Layer V stains lightly, both in patch and in interpatch tissue. **G** Deep in layer VI, the overall staining is slightly higher than in layer V, but patches are not clearly defined

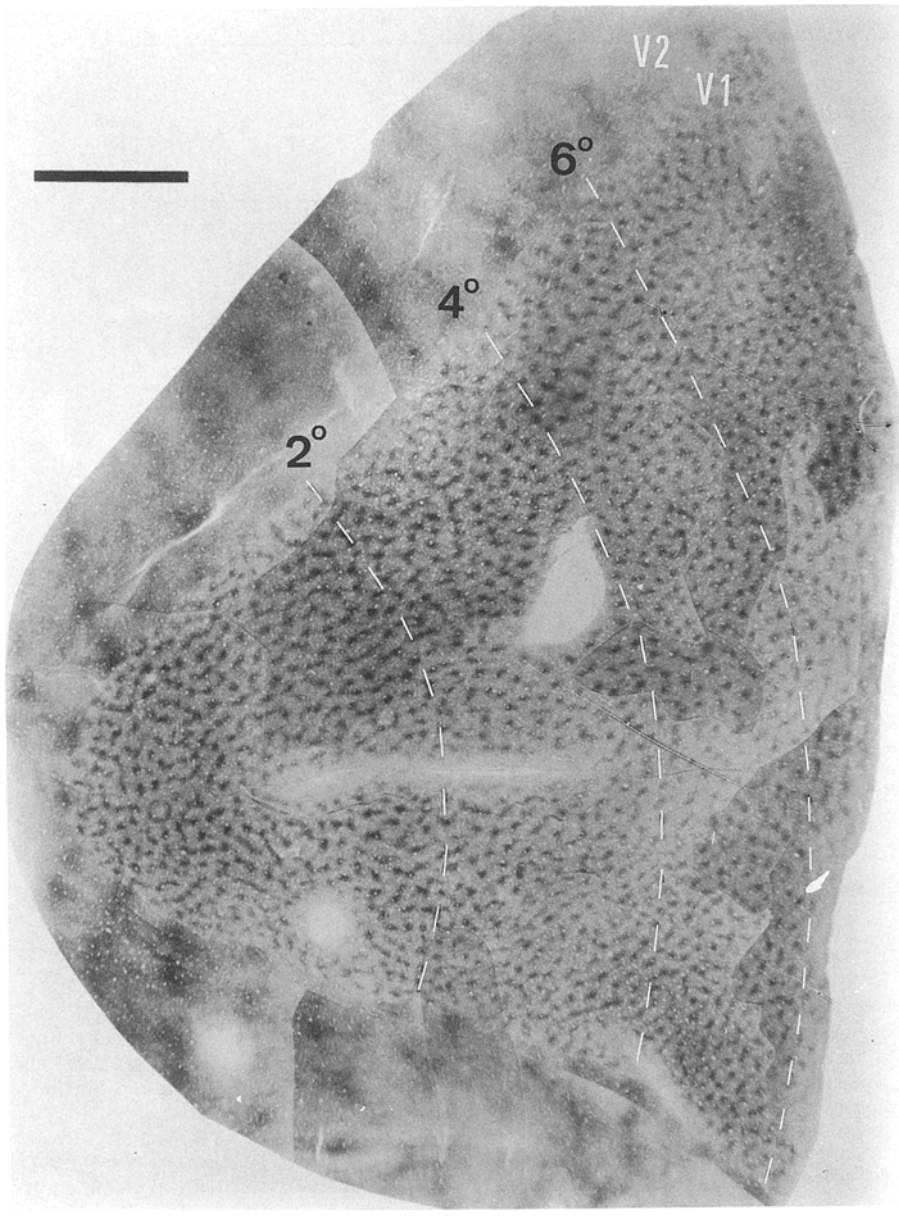

Fig. 3. Photographic montage showing the pattern of cytox-rich patches in the occipital operculum of one monkey (CO4L). Foveal is leftwards. The representation of the lower visual quadrant is upwards, and that of the upper quadrant is downwards. Three isoeccentricity lines are shown dashed. Note also the cytox banding pattern in V2. Scale bar = 5 mm

in the macaque (Horton 1984; T'so and Gilbert 1988), but they are far less clearly separated than those of the squirrel monkey (Horton 1984).

In general, the highest contrast between patch and non-patch tissue is observed at the foveal representation (Fig. 3). At more peripheral locations, patch borders are fuzzy (see also Fig. 1). Furthermore, bridges linking adjacent patches are more frequent at the foveal representation (Figs. 1 and 3).

Patch spatial densities

Figures 1 and 3 also illustrate that, in the *Cebus*, the number of patches per mm^2 is fairly constant throughout V1. The number of patches per mm^2 at the representation of different eccentricities and polar angles in V1 is shown in Fig. 4. In each case, the number of patches/mm^2 shows little variation along the polar sectors considered. Moreover, whenever present, the tendency of the variation is not consistent among different polar sectors or different monkeys: For example, the number of patches/mm^2 increases significantly ($P < 0.01$) with increasing eccentricity along the lower vertical meridian in case CO7, but not in CO4 or CO10. Averaging across animals, there is no significant variation of patch spatial density with eccentricity. Notwithstanding, a significantly smaller (smallest t value among three cases = 3.8, $P < 0.01$) patch density was observed at the monocular periphery as compared to neighbouring portions of the binocular field (Figs. 4 and 12).

Patch spatial density varied significantly among individuals. Although monkeys with large striate cortices tend to show less patches/mm^2, there is no simple inversely proportional rule between patch density and the size of V1 (Table 1, see also Fig. 12). For example,

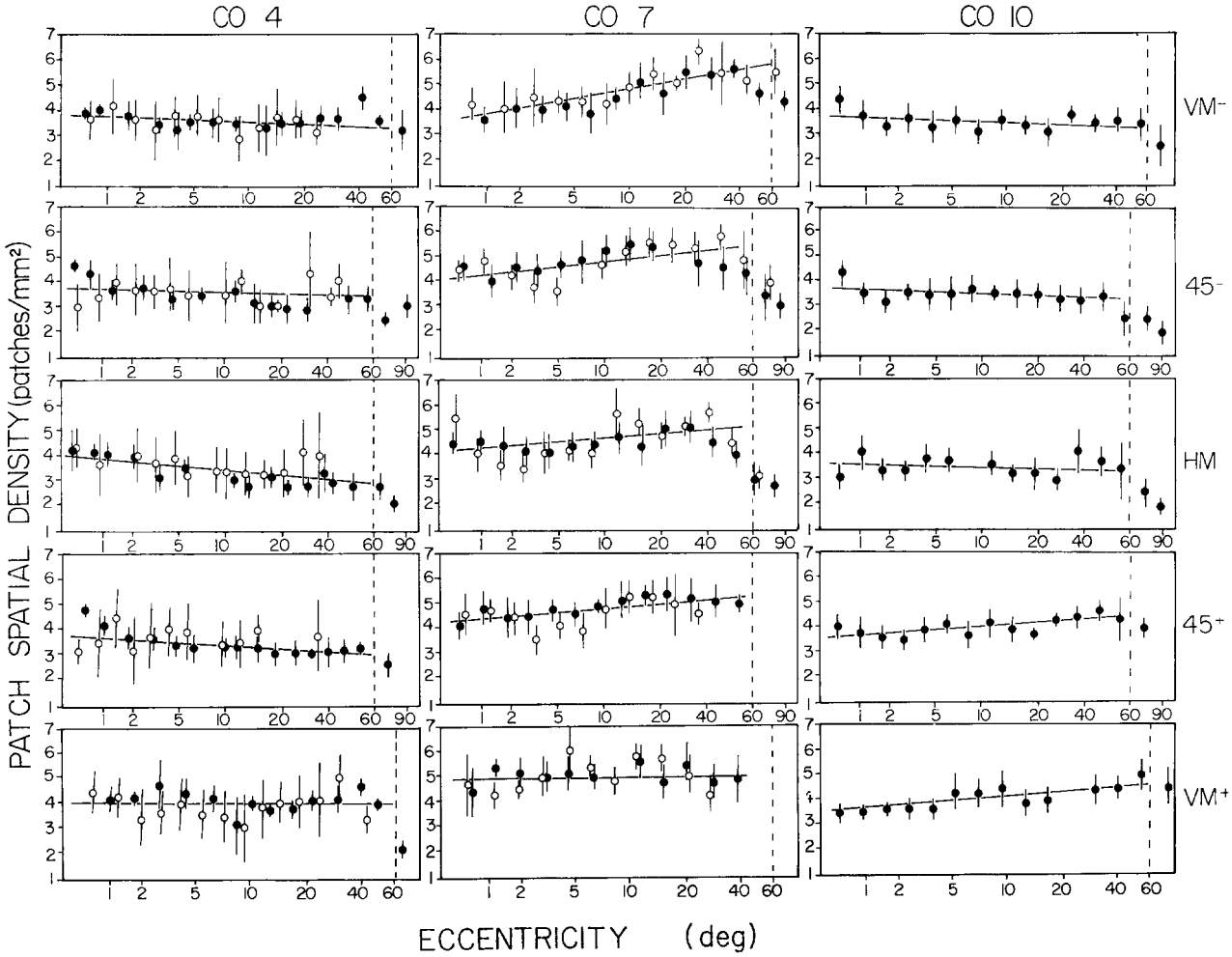

Fig. 4. Patch spatial density as a function of eccentricity in 3 animals. Five polar angle sectors are illustrated, one at the horizontal meridian (HM), 2 below (45- and lower vertical meridian, VM-) and 2 above (45+ and VM+). Each datum point is the mean +/−1 standard deviation of counts made in at least 8 adjacent 1 mm² sectors. *Circles* correspond to measurements in right hemispheres, and *dots* to left hemispheres. In each case, a straight line was fitted to the data along the presumptive binocular field. The *vertical dashed lines* indicate the approximate location of the inner border of the monocular field

Table 1. Patch density and patch area vs area of V1

Hemisphere		Area of V1 (mm²)	Patches/mm²[a]	Patch area[a] (mm²)
CO4	left	1307	3.60 (+/−0.25)	0.044 (+/−0.008)
	right	1216	3.64 (+/−0.27)	
CO7	left	748	4.75 (+/−0.56)	0.034 (+/−0.005)
	right	761	4.79 (+/−0.66)	
CO10	left	1502	3.72 (+/−0.17)	0.053 (+/−0.008)

[a] Mean and standard deviation of sectors located in the binocular field

although the surface of V1 in CO10L is about 15% larger than that of CO4, there is no significant difference ($0.5 < P < 0.55$, $t = 0.67$) in patch spatial density between these monkeys.

Patch cross-sectional area

Figure 5 shows that, except in the neighborhood of the horizontal meridian representation, there is a small but consistent decrease of patch cross-sectional areas with eccentricity within the representation of the binocular field (see also Fig. 12). In addition, a significant (smallest t among 3 cases $= 3.61$, $P < 0.01$) increase in patch area is observed at the transition between binocular and monocular field representation (Figs. 1 and 5). The fact that this increase is not apparent for all polar sectors is probably due to two factors. First, there is an imprecision in delimiting the exact boundary of the monocular field based on magnification factors and, therefore, there may exist some contamination from binocular field patches in the sample. Second, the extent of the monocular crescent varies somewhat among individuals (unpublished observations) and among polar angles, being widest at the horizontal meridian. Averaging across polar sectors, the shape of the curve relating patch area and eccentricity is the same across individuals (Fig. 12).

There is also a significant variability in patch area among individual monkeys. In larger striate cortices (CO4, CO10) the mean patch areas are proportionally higher than in smaller ones (CO7, see Table 1 and Fig. 12).

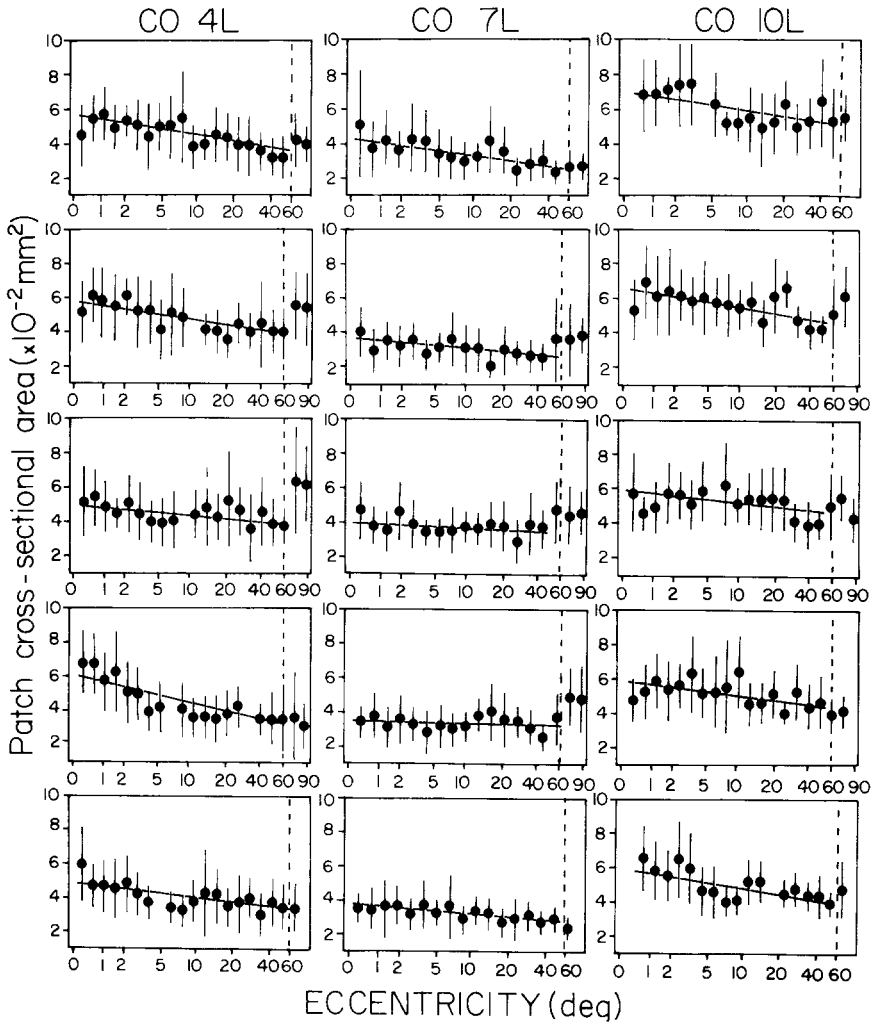

Fig. 5. Patch cross-sectional area as a function of eccentricity along 5 isopolar sectors of 3 animals (left hemispheres only). Five polar sectors, ranging from the vicinities of the lower vertical meridian *(upper line)* to the upper vertical meridian *(lower line)* are shown arranged as in Fig. 4. A straight line was fitted to the data along the presumptive binocular field representation. The approximate eccentricity of the inner limit of the monocular field is shown as a *dashed line*. Each datum is the mean +/− standard deviation of the area of at least 20 patches

Within the binocular field representation, as a result of the near constancy of patch spatial density and of the small decrease of patch area with increasing eccentricity, the fraction of V1 surface corresponding to cytox patch tissue tends to decrease towards the periphery. Patches correspond to about 20% of the surface at foveal V1, and to about 15% at the border of the binocular field. At the monocular field representation, patches correspond to only 12% of the surface of V1.

Patches in monocularly enucleated monkeys

In monocularly enucleated *Cebus* monkeys, cytox patches overlying deprived ocular dominance stripes are smaller than at their undeprived counterparts (CO5R, $t=8.83$; CO5L, $t=12.57$; CO6R, $t=20.21$; $P<0.0001$ in all cases). This difference can be, at least in part, attributed to light staining of the deprived eye dominance columns (Hess and Edwards 1987). In view of this difference, the tendency of cytox patches to form rows along ocular dominance stripes stands out better in enucleated than in normal animals (Fig. 6). As expected, it is particularly difficult to delineate patches corresponding to the enucleated eye in most cortical layers (Fig. 7), due to the shrinkage of these patches and to the low contrast between patches and surrounding tissue.

In macaques, it has been reported that patches from the enucleated eye tend to shrink, thus accounting for the observed difference in patch area (Trusk et al. 1990). In the *Cebus*, however, if one compares mean patch area at stripes corresponding to the remaining and the enucleated eye with normal controls, one is led to conclude that not only patches of the enucleated eye shrink, but also patches of the intact eye expand. This point is illustrated in Fig. 8, which compares patch area at retinotopically corresponding loci in V1 in normal and enucleated monkeys. Both the shrinkage of patches corresponding to the enucleated eye and the enlargement of patches corresponding to the intact eye are clearer if one compares patch size of enucleated cases with controls matched for V1 area (vertical dashed lines in Fig. 8). If such a comparison is made, both the shrinkage of deprived patches and the enlargement of undeprived ones are significant to $P<0.0001$ (CO5R deprived × CO10L, $t=5.2$; CO5R undeprived × CO10L, $t=3.85$; CO5L deprived × CO10L, $t=8.14$; CO5L undeprived × CO10L, $t=4.37$; CO6R deprived × CO4L, $t=11.29$; CO6R undeprived × CO4L, $t=7.24$). Therefore, the expansion of the patches corresponding to the remaining eye is

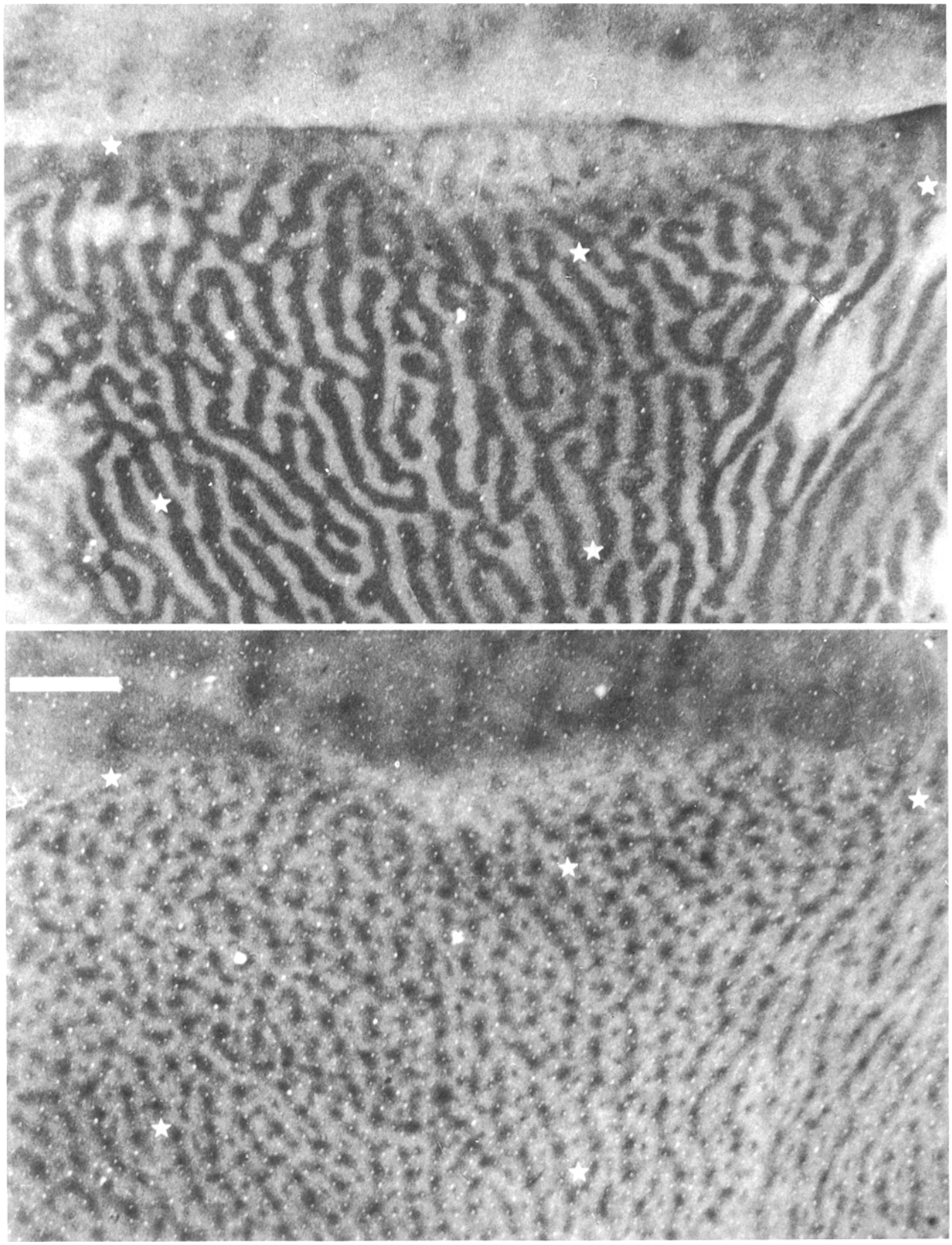

Fig. 6. Effect of monocular enucleation on the rows of cytox patches in V1. *Upper:* low-power view of the pattern of ocular dominance stripes in layer IVc of V1 of a monkey sacrificed 4 months after monocular enucleation (CO6R), as revealed by cytox staining. *Lower:* a section mostly through layer III of the same sector of V1, showing the formation of rows of alternately large and small patches. These photographs correspond to the representation of the central lower quadrant in V1, close to the representation of the vertical meridian. Note the pattern of fuzzy cytox bands in V2, at the upper portion of each photograph. A set of corresponding blood vessels is marked by stars to aid in localization. Scale bar = 2 mm

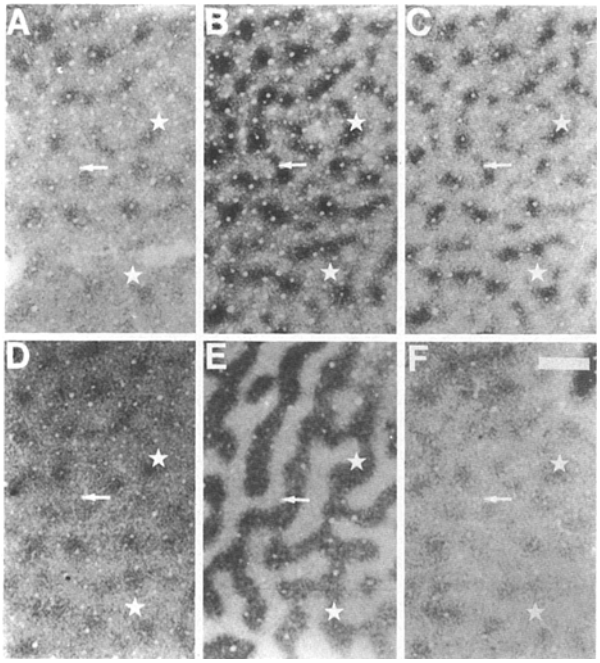

Fig. 7A–F. Effects of monocular enucleation in different cortical layers of V1. **A–F** Are sections from layer II, middle layer III, lower layer III, layer IVb, IVc-beta and V, respectively, taken from an animal enucleated 7 months before sacrifice (CO5R). They correspond to an eccentricity of about 3° in the lower visual field. In sections **A, D** and **F**, patches corresponding to stripes of the intact eye are very large, while enucleated eye patches are barely distinguishable from interpatch tissue. In sections **B, C**, patches appear with high contrast. Patches correspondig to both eyes are largest and darkest in middle layer III (section **B**) than elsewhere. Section **E** shows the corresponding eye dominance stripes in layer IVc-beta. A pair of blood vessels is labeled with stars to aid in localization, and an arrow points to an example of confluent patches overlying enucleated and remaining eye stripes. Scale bar = 1 mm

significant both in the 4 months-enucleated monkey (CO6) and in the 7 months-enucleated one (CO5). In case CO5, the variance of patch area along undeprived stripes is also larger than that of normal controls. It should be pointed out that we used a purely morphological approach in defining the cytox patches, and have no data concerning possible changes in functional properties. Therefore, it would be equally appropriate to say that the interpatch tissue around patches corresponding to the intact eye increases its cytox reactivity, becoming indistinguishable from the original patch, as suggested by Hendry et al. (1988).

Patches along intact-eye ocular dominance stripes become almost confluent (Fig. 6) for most of V1. We considered the possibility that the increment in patch area is brought about by fusion of adjacent patches, inasmuch as we observed several instances in which deprived and undeprived patches were essentially continuous (see arrow in Fig. 7). The data on patch density, however, do not support this hypothesis: patch densities at the studied sites are not reduced as compared with normal animals.

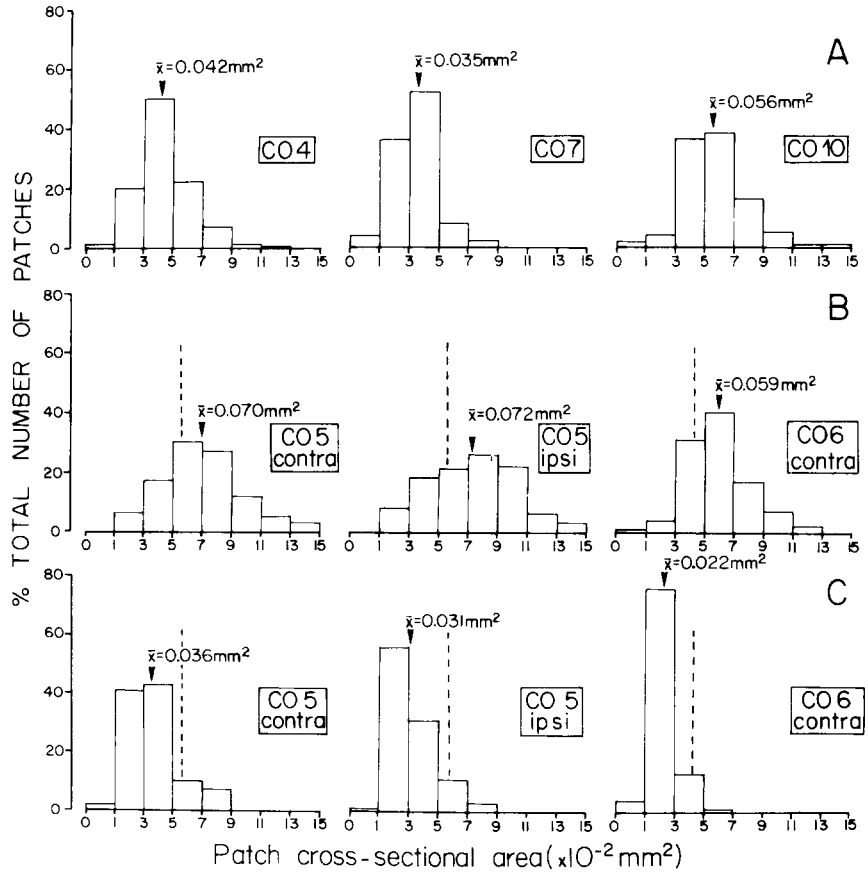

Fig. 8A–C. Distribution of patch area at comparable locations in V1 of normal and monocularly enucleated monkeys. All measurements correspond to a sector along the horizontal meridian at about 4° eccentricity. **A** Three normal animals. **B** Patches located along intact-eye stripes in two enucleated monkeys. **C** Patches located along enucleated-eye stripes. Note that there is no difference between the mean area of patches measured in the hemispheres contralateral and ipsilateral to the enucleated eye in CO5. The vertical dashed lines in **B, C** indicate mean patch area in normal controls roughly matched for VI size: CO5 (mean VI area of 2 hemispheres = 1496 mm²) is compared with CO10L (1502 mm²), while CO6R (1290 mm²) is compared with CO4L (1307 mm²)

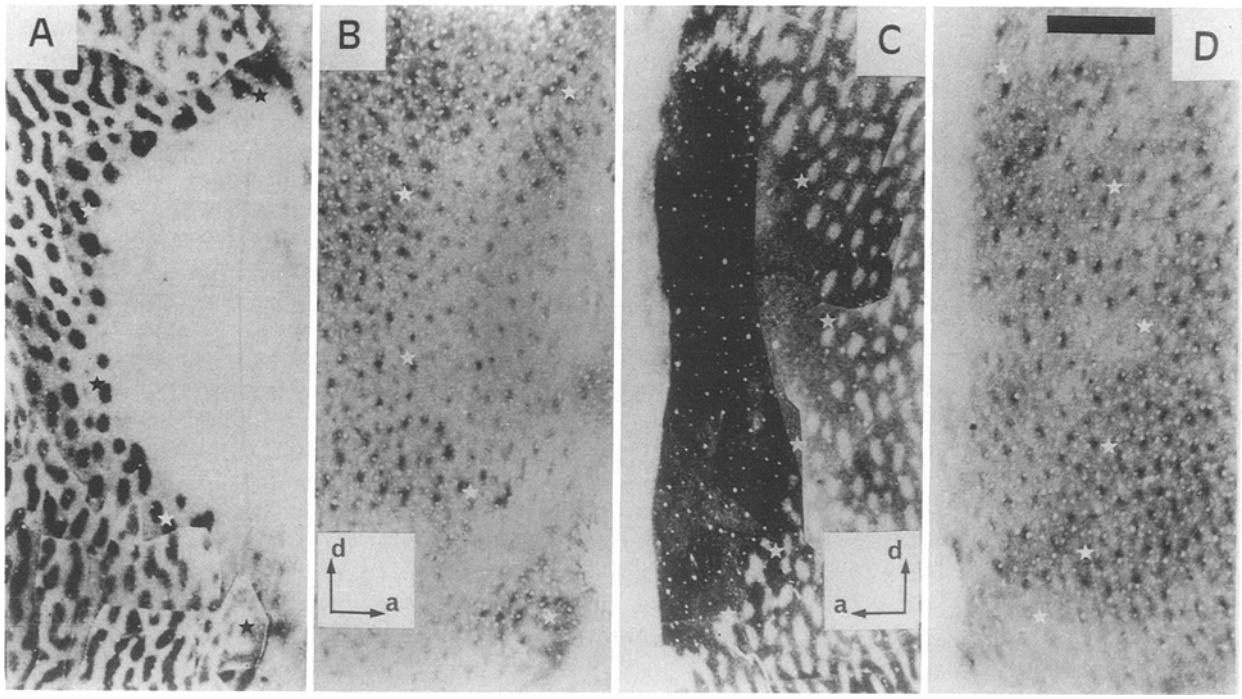

Fig. 9A–D. Effect of monocular enucleation on cytox patches at the representations of monocular crescents. **A** Photographic montage of sections through layer IVc, showing the extent of the representation of the monocular crescent of the enucleated eye (large territory of homogeneously light staining delineated by stars). **B** A section through layer III, showing that cytox patches survive long-term enucleation (7 months, in this case). **C** Montage showing the extent of the monocular crescent representation of the remaining eye (dark region circumscribed by stars). **D** A section through layer III, showing the patches overlying the monocular sector shown in **C.** The stars label the same radial blood vessels in **A** and **B,** and in **C** and **D.** Scale bar (all photographs) = 3 mm: "d" indicates dorsal, and "a", anterior in the calcarine sulcus

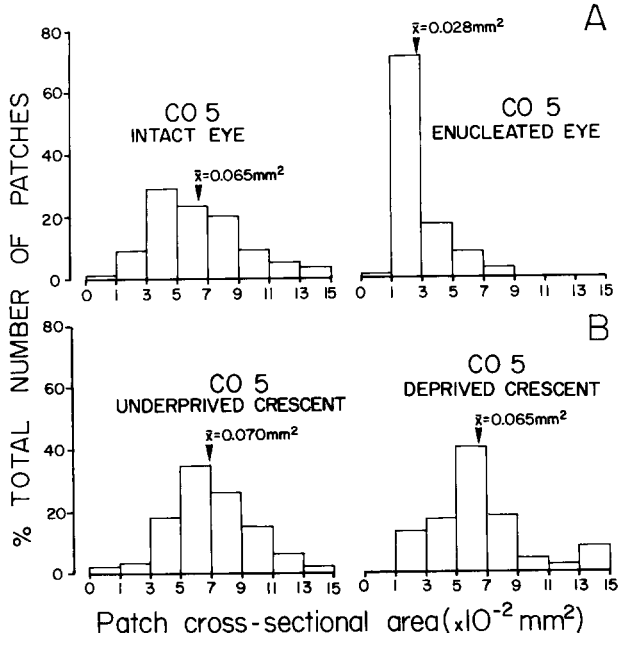

Fig. 10A, B. Effect of enucleation on cytox patches subserving peripheral vision. **A** Patch areas at the border of the binocular field. These measurements represent both hemispheres of CO5, and were made on sectors extending to 5 mm around the border of the monocular fields. These distributions show a deprivation effect similar to that observed at more central locations (Fig. 8). **B** Patch sizes in the undeprived and deprived monocular sectors of V1

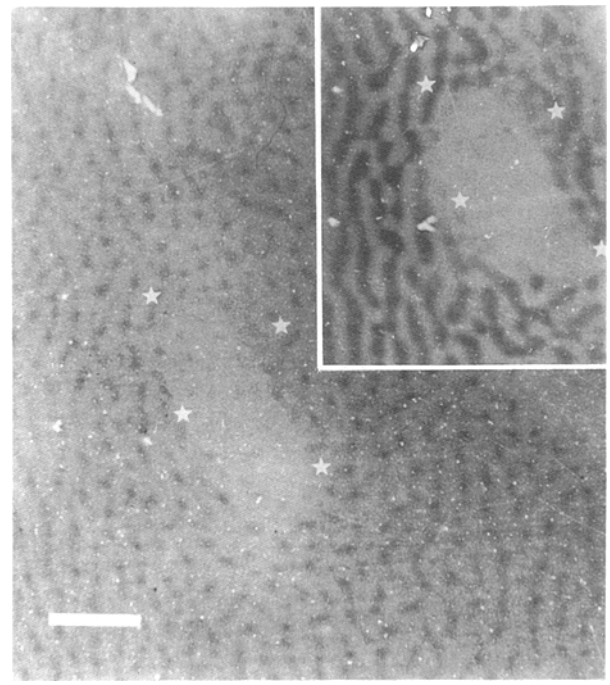

Fig. 11. Effect of monocular enucleation at the region of V1 corresponding to the optic disk of the contralateral (remaining) eye. Note that in the optic disk sector (roughly delimited by the stars) patches are barely visible. This section corresponds to the middle portion of layer III, where patches are clearest. Insert: Extent of the optic disk sector in this hemisphere, as shown in a section through layer IVc. Stars label the same blood vessels for orientation. Scale bar = 2 mm. for both photographs

Figure 9 shows the pattern of patches in the deprived and undeprived monocular crescent representations in the 7 months enucleated monkey. In this case, patch areas are not statistically different ($t=0.91$, $0.4<P<0.45$, see Fig. 10), in spite of the lighter staining in the hemisphere contralateral to the enucleated eye, which involves both patch and non-patch tissue (Fig. 9). Even after 7 months of complete deprivation, cytox patches are well delimited in the monocular crescent.

In this case (CO5), it was possible to calculate the precise values of patch density in the representation of the monocular crescent, by using layer IVc as a reference to the limits of the binocular field. The patch density came out to be 2.1 and 2.2 patches/mm^2 in the deprived and undeprived crescents, respectively. Therefore, there is no loss of patches in long-term deprived monocular territories. These values are somewhat lower than those obtained from normal animals (mean, 2.9 patches/mm^2), but this difference might reflect the uncertainty in the determination of the boundaries of the monocular representation in these cases.

The cortical sector of V1 which corresponds retinotopically to the blind spot of the contralateral eye is located in the triangular-shaped "roof" of the calcarine sulcus (Gattass et al. 1987; Rosa et al. 1988b). In Fig. 11 it is possible to observe that patches become extremely faint in this region after 4 months of enucleation. This observation was confirmed in the 7 months enucleation case. In fact, they are detectable very faintly and only at the middle of layer III (Fig. 11). Averaging across three blind spot sectors (two enucleated, one non-enucleated), we found that this portion of V1 shows a low patch spatial density (mean, 2 patches/mm^2) as compared with the surrounding tissue.

Discussion

Comparison with previous studies

Cytochrome oxidase-rich patches were previously investigated in V1 of *Cebus* by Hess and Edward (1987), who analyzed the occipital operculum of a single specimen. These authors report a mean patch area value of 0.05 mm^2, and a mean patch density of 3.45 patches/mm^2. These values are very close to the ones we report for the larger animals is this paper, in spite of the different methods employed in tissue processing and in the quantitative analysis. Hess and Edwards (1987) also noticed, in agreement with our results, that the rows of patches in V1 are shorter in the *Cebus* than in Old World monkeys. We also observed that patches tend to be individualized in *Cebus*, with few obvious bridges of cytox-reactive tissue between them. This tendency may account for the less conspicuous arrangement in rows, inasmuch as ocular dominance stripe topography is similar in both *Cebus apella* and *Macaca fascicularis* (compare, for example, Rosa et al. 1988b and Tootell et al. 1988a). Moreover, we observed a variability among monkeys and among different regions of V1 with respect to the regularity of the ocular dominance banding pattern (Rosa et al. 1988b, and in prep.). For example, as in most macaques, in the case shown in Fig. 6 both ocular dominance stripes and patch rows are long and run parallel to each other for a large extent.

Cytochrome oxidase patches in other species of monkey

Horton (1984) noticed, in the macaque, an increase in patch density with eccentricity within the representation of the binocular field. In one of his cases (Fig. 42 in Horton 1984) patch density reached 9 patches/mm^2 at the border of the monocular field, while values at the occipital operculum, i.e., at the representation of central vision, were about 5 patches/mm^2. An increase in patch density with eccentricity in macaques was also reported by Livingstone and Hubel (1984), who studied the representation of the central 10 degrees of the visual field. By contrast, patch density in *Cebus* is nearly constant

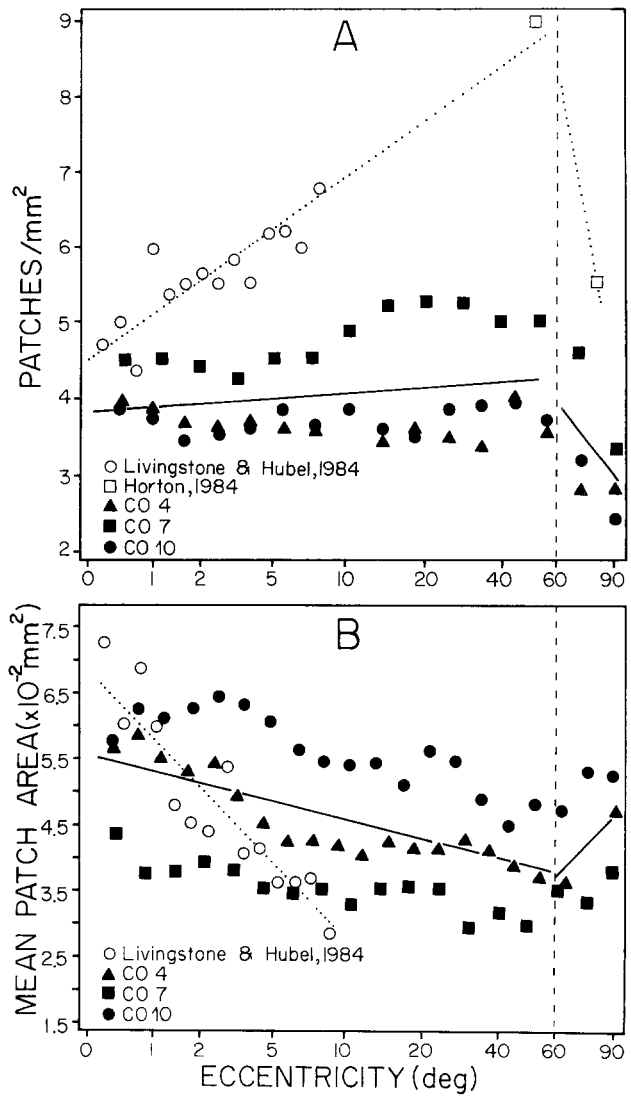

Fig. 12A, B. Comparison of patch density **A** and patch cross-sectional area **B** in *Cebus apella* and *Macaca fascicularis*. In both cases, straight lines were fitted in order to express the mean variation of the data with eccentricity

throughout the binocular field. In spite of individual variability, we never observed a twofold increase in patch density, as in macaques (Fig. 12A). Therefore, we are confident that this unexpected difference between *Cebus apella* and *Macaca fascicularis* is real, in spite of the similarities of V1 of these species with respect to size, cortical magnification factors and sulcal patterns (Gattass et al. 1987).

Similarly to Horton (1984), in this paper we report an abrupt decrease in patch spatial density at the transition from binocular to monocular representation in V1 (Fig. 12A), although the reported value for *Macaca fascicularis* (5.5 patches/mm^2) is somewhat higher than that for *Cebus* (2.1–3.9 patches/mm^2). It is reasonable to conclude that this different spatial distribution of patches in the binocular vs monocular field might be related to the absence of ocular dominance stripes.

With regard to other New World monkeys, there are interspecies differences relative to patch size, density and regularity of distribution. In the squirrel monkey, Horton (1984) found the patches to be rounder, smaller and more clearly separated than those of macaques. Analysis of his illustrated case (Fig. 14, Horton 1984) shows that these differences also apply to a comparison between *Saimiri* and *Cebus*. The regular distribution of patches in *Saimiri*, which follow a square or hexagonal grid, also contrasts with the pattern found in *Cebus* (Fig. 3). However, the clear separation and the regular distribution of patches are characteristics of cytox patch topography in *Callithrix jacchus*, the marmoset (manuscript in prep.), suggesting that this may be a characteristic of small New World monkeys, which lack ocular dominance columns (Rosa et al. 1988b). With regard to patch density, the present estimates in *Cebus*, Horton's (1984) estimates in *Saimiri* (4.5 patches/mm^2) and our estimates in *Callithrix* (about 6.0 patches/mm^2, manuscript in preparation) suggest that patches are compressed in the smaller species. Note, however, that the surface of striate cortex in the marmoset is about one-fifth of that in *Cebus*, while patch topography is not proportionally compressed. This result leads one to conclude that the organization of striate cortex in small monkeys is not a simple compression of that found in the large ones. The data on patch density may also imply in differences between New and Old World monkeys, since the macaque shows a high patch density which, especially in the peripheral representation, is even higher than that of the marmoset, in spite of its large striate cortex. Moreover, data illustrated by Cusick and Kaas (1988, Fig. 2) and by Tootell et al. (1985) suggest that in squirrel and owl monkeys, as in the *Cebus*, patch density may not increase towards the peripheral representation. If it is assumed that cytox patches are reliable markers of cortical modules (see below), one would also conclude that the size of these modules is nearly invariant in New World, but not Old World monkeys.

An unusual New World monkey, in terms of its patch topography, is the nocturnal owl monkey, *Aotus*, that shows a relatively low patch density (1000 patches in about 400 mm^2 = 2.5 patches/mm^2, Tootell et al. 1985) with respect to the size of V1. Cytochrome oxidase patches in owl monkeys are also different because they are visible in all cortical layers, including layer IVc. Inasmuch as the current evidence suggests that the earliest Simiiforms were diurnal (Hoffstetter 1982; Fleagle 1988), these departures from the rule are almost certainly autapomorphic and linked to the nocturnal/crepuscular habits of these unique simians (Wright 1981).

We found a small decrease of patch size in V1 with increasing eccentricity, which is not observable at the horizontal meridian representation. This decrease is far more evident in macaques than in *Cebus* (Fig. 12B), a fact that is probably related to the larger variation of patch density found in the former (Livingstone and Hubel 1984). Similarly to Trusk et al. (1990), we observed that patches tend to be largest in the middle portion of layer III (see Figs. 2 and 7).

Cytochrome oxidase patches and cortical modules in V1

In VI of *Cebus*, as in the macaque, cytox patches are in register with ocular dominance stripes (Horton and Hubel 1984; Hess and Edwards 1987). Therefore, each cortical module must encompass a minimum of two cytox patches. Based on this assumption and on an estimate of 4 patches/mm^2, one would expect that the tangential spread of activity elicited by the stimulation of a point of the visual field would cover about 0.5 mm^2 for most of V1. This figure comes close to the electrophysiologically determined point image area at the peripheral representation of V1 but it is several times smaller than that at the central representation (Gattass et al. 1987). Recent evidence, however, suggest that this may be an oversimplified view of the relationship between patch spatial density and cortical point images. T'so and Gilbert (1988) studied the central visual field representation in V1 of macaques, and showed that cytox patches are usually of two different types, i.e., the patches which encompass neurons selective to red/green (RG) color contrast and those containing blue/yellow (BY) selective neurons. These types of patches seem to occur in a 3 : 1 ratio in central V1. In addition, a third type of cytox patch may exist, containing neurons responsive to broadband (BB) stimuli. Therefore, for a cortical point image in central V1 of macaques to contain all the neuronal machinery for the analysis of a given point of the visual field, it must be composed by at least 8, and possibly 10 or more cytox patches (3 RG : 1 BY : 1 BB patches × 2 eyes), occupying about 2 mm^2, in closer agreement with the estimates of the central point image area. In this model, point images in V1 would vary as a function of the relative numbers of RG, BY and BB patches at different eccentricities. At the monocular representation one might predict the existence of a single type of patch. This model can be tested by correlating point image areas along an isopolar line moving towards the peripheral representation of V1 with the relative proportions of RG, BY and BB patches.

Another model, by Schein and de Monasterio (1987), proposes that cytox patches in V1 at all eccentricities receive input from a constant number of lateral geni-

culate nucleus (LGN) parvicellular (P) layer cells, but not magnocellular (M) layer cells. In this model, the decrease of point-image area with increasing eccentricity in V1 would result from the different slopes of the magnification function of P and M LGN layers. Schein and de Monasterio suggested that M projections to V1 would be sparser centrally than peripherally. As a consequence, in order to keep a single visuotopic map, the ratio of receptive field size in M- vs P-dominated regions in V1 would be larger centrally than peripherally. The relatively large central receptive fields would raise the central point image area. This model also embodies a clear prediction for *Cebus*, which remains to be tested, namely, that the magnification factor in LGN P layers and in V1 would vary as a function of eccentricity following functions with similar slopes, in view of the nearly constant patch density in this species. In contrast, the magnification factor at LGN M layers would decrease much less steeply than that of V1.

It is also important to keep in mind, at this point, that recent estimates of point image size in V1 are different from those evaluated by electrophysiological recordings, suggesting that cytox patch topography may have a more direct relationship with the way the visual field is divided for analysis by modular components of V1. Tootell and collaborators (1988b), who used the 2-deoxyglucose metabolic mapping method, reported values of point image size that are several times smaller than those proposed by Dow et al. (1981) by electrophysiological recordings. It could well be, therefore, that at any given moment only part of the total number of possible processing pathways in V1 is used to analyse a region of the visual field. The large point-images of central V1, as evaluated by electrophysiology, could reflect in part the dynamics of receptive field position along time (Motter and Poggio 1982). Changes in receptive field extent in V1 are also predicted by the model of Anderson and Van Essen (1987), and were recently demonstrated in *Cebus* monkeys (Fiorani et al. 1990). Moreover, the electrophysiological studies so far published did not distinguish between the contribution of geniculate afferents and that of "backward" prestriate projections to V1 (Gattass et al. 1990b) in determining receptive field size in the latter. If prestriate projections do contribute to receptive fields in V1, then anatomical tracer studies, such as those of Livingstone and Hubel (1988) may prove to be more adequate than electrophysiological studies to reveal the quantitative relationships in the pattern of interconnections from retina to cortex. From this viewpoint, patch topography could have a more direct relationship with the pattern of geniculocortical projections as well.

Increase in patch areas along undeprived-eye stripes

In monocularly enucleates specimens, we observed that cytox patches in undeprived stripes tended to be larger than in the deprived ones, thus confirming the results of Hess and Edwards (1987). Moreover, our data showed that patches of the intact eye in *Cebus* are larger than patches from normal controls matched for V1 size. Based on the current evidence, we cannot rule out the possibility that the larger patch areas observed in the enucleated cases only reflect individual variability and that undeprived patches simply do not change in size after their counterparts' deprivation. Certainly, a more rigorous experiment comparing patch area before and after enucleation in the same individual is needed to settle this question. It might be possible, for instance, in chronic experiments to map the same region of V1 with voltage-sensitive dyes (Blasdel and Salama 1986) in these two conditions. This experiment would require the functional properties of neurons around the patches of the remaining eye to change in parallel with their cytox reactivity, so that a specific stimulation could reveal both the original patch and the new cytox-rich "ring" of tissue. There is, at present, no evidence to support the existence of such changes. It could also be that the apparent enlargement of cytox patches corresponding to the remaining eye is simply a consequence of the lowering of cytox reactivity in the deprived eye stripes, resulting in a large contrast between deprived and undeprived interpatches that would mask the differences between undeprived patches and interpatches. For several reasons, we regard this as unlikely. First, enlargement of patches in noticeable in the peripheral representation, a region of V1 where patches do not form continuous rows even after long post-enucleation survival times (Figs. 9 and 10). Second, the enlargement is visible in all layers of V1, even in those where there is no difference between deprived and undeprived interpatches (Fig. 7). In Figures 6 and 7, it is also possible to observe that interpatch tissue is differentiable from patch tissue along intact-eye stripes, an impression that was confirmed by computer scans.

In spite of the above mentioned possible limitations of our analysis there are good reasons to suspect, at this point, that the size increase of the patches in undeprived stripes is real. First, the patches in undeprived stripes form almost continuous rows, differently from those at corresponding portions of V1 in normal monkeys. Second, Horton's (1984) description in a *M. fascicularis* monocularly enucleated for six months, seems to indicate similar observations: "patches in dark rows appear larger and semi-confluent" (shown in Fig. 28, Horton 1984). This author also noticed that patches tended to become confluent after long periods of monocular lid suture. Hendry et al. (1988) also observed an increase in patch area after monocular lens removal for six months, but not after 15 days of deprivation with intravitreal tetrodotoxin injections. Although the latter study attributed this difference to the specific effects of these experimental manipulations, the critical variable may have been, in fact, the survival time. In the *Cebus*, the shrinkage of the deprived patches was visible even in the 18 day-enucleated monkey, while an increase in the patch area along undeprived stripes was only clear after several months of enucleation. Although the planes of section were not adequate for analysis of patch size in case CO11, there is a suggestion of the formation of more clear rows in undeprived stripes in this case. The results obtained in *Cebus* are in some aspects comparable to those reported by Trusk et al. (1990) for macaques sub-

mitted to either monocular enucleation or injections of tetrodotoxin. For example, in both *Cebus* monkeys CO5 and CO6 patches corresponding to the enucleated eye were 50–60% smaller than those corresponding to the intact eye, while the difference in cross-sectional areas seemed less marked in CO11. In the macaque, the difference between deprived and undeprived patches proved to be smaller in monkeys sacrificed 2 weeks after the onset of the monocular treatment than in monkeys allowed to survive for longer times, in which the difference also amounted to 50–60%. The aspect of cytox patch rows in a *M. fascicularis* enucleated for about 7 months was also similar to that observed in the *Cebus* after a similar survival time (Fig. 2c of Trusk et al. 1990).

A model of the plastic mechanisms involved in patch enlargement

The present results suggest that, under conditions of ocular imbalance, the "periblob" regions (Livingstone and Hubel 1984; T'so and Gilbert 1987), which contain neurons with intermediate degrees of orientation selectivity and ocular dominance, may increase their cytox reactivity. Electron microscopic evidence shows that cytox reactivity in the patches of V1 is predominantly localized within dendrites (Carrol and Wong-Riley 1984). In a quantitative study of cytox reactivity in striate cortex of macaques which underwent chronic monocular blockage with tetrodotoxin, Wong-Riley and collaborators (1989) demonstrated that the greatest changes in neuropil reactivity occurs at the borders of patches. In this region, axon terminals forming asymmetrical synapses become less densely packed around dendrites after long inactivation times. Wong-Riley et al. (1989) suggested that these terminals may be in part replaced by axonal sprouting of terminals forming symmetrical synapses, which in normal animals contain several highly cytox-reactive mitochondria. Based on these data and on the working model of Wong-Riley et al. (1989), one may envisage a model to explain the increase in undeprived patch area after long periods of monocular enucleation. Inasmuch as interpatch tissue contains neurons which respond to both eyes, it is likely that monocular enucleation promotes functional rearrangements in this region also. In regions immediately outside the undeprived patches, terminals of neurons dominated by the enucleated eye may be replaced by terminals of neurons dominated by the intact eye. If there is also a preferential replacement of asymmetric by symmetric contacts (as it is likely to occur at the border of deprived patches), one would expect an overall increase of cytox reactivity around the patches, since symmetric synapses show high cytox reactivity. In the absence of ultrastructural evidence, this rather speculative model give a possible explanation for increments in undeprived patch areas, and emphasizes that such an increment could be brought about without any need for still undescribed mechanisms. Moreover, it emphasizes that the apparent enlargement of patches in likely to be related to plastic mechanisms involving neuropil rather than cell bodies.

Patch plasticity in monocular sectors of V1

A novel observation of this study regards the patch size in the representation of the monocular crescents. Deprived and undeprived crescents show no difference in patch size, a result which contrasts with the marked difference observed between ocular dominance stripes in binocular V1. These results suggest that changes in patch size may result from competition between inputs coming from each eye, rather than from the absolute amount of activity driven by each eye separately. This last factor may be at the basis of the difference in the overall intensity of cytox stain in deprived and undeprived crescents. In the macaque, Horton (1984) found cytox patches in both monocular crescents of a monkey that had been monocularly deprived by lid suture for 6 months. Although Horton's study provides no measurements of patch area in these regions, we were unable to detect any gross difference between deprived and undeprived crescents in his illustrated case (Fig. 42 of Horton 1984). On the other hand, deprivation-related changes in patch topography were clear in the same monkey within the binocular representation (Figs. 41 and 42, Horton 1984). Therefore, one can conclude that deprivation-related changes in the patches subserving the monocular crescents are less severe than those in the binocular field representation, both in New- and Old World monkeys. Interestingly, the other monocular region of striate cortex, i.e., the retinotopic region corresponding to the optic disk, is severely affected by enucleation, as far as cytox reactivity is concerned (Fig. 11). Studies in our laboratory are underway to explain this puzzling difference.

Acknowledgements. Dedicated in memoriam to Gal. Armando Batista Gonçalves, a constant source of stimulus and inspiration. The authors would like to acknowledge Drs. C.E. Rocha-Miranda and A.P.B. Sousa sor critical reading of the manuscript, M. Fiorani Jr. for computer programming, and L.A. Cavalcante for help with the cytox histochemistry procedure. This work would not be possible without the aid of E.S. da Silva Filho in photography, of V.P.G.P. Rosa in histology and artwork, and of P.C. and G. Coutinho in animal care and preparation. We are also indebted to the Função Parque Zoológico de São Paulo for the donnation of the monkeys. Supported by grants from FINEP, FAPERJ, CNPq, and IBM Brasil.

References

Anderson CH, Van Essen DC (1987) Shifter circuits: a computational strategy for dynamic aspects of visual processing. Proc Natl Acad Sci USA 84:6297–6301

Blasdel GG, Salama G (1986) Voltage-sensitive dyes reveal a modular organization in monkey striate cortex. Nature 321:579–585

Carrol EW, Wong-Riley MTT (1984) Quantitative light- and electron microscopic analysis of cytochrome oxidase-rich zones in the striate cortex of the squirrel monkey. J Comp Neurol 222:1–17

Cusick CG, Kaas JH (1988) Cortical connections of area 18 and dorsolateral visual cortex in squirrel monkeys. Vis Neurosci 1:211–237

Dow BM, Snyder AZ, Vautin RG, Bauer R (1981) Magnification factor and receptive field size in foveal striate cortex of the monkey. Exp Brain Res 44:213–228

Fiorani Jr. M, Gattass R, Rosa MGP, Sousa APB (1989) Visual area MT in the *Cebus* monkey: location, visuotopic organization and variability. J Comp Neurol 287:98–118

Fiorani Jr. M, Gattass R, Rosa MGP, Rocha-Miranda CE (1990) Changes in receptive field size of single cells in primate V1 as a correlate of perceptual completion. Soc Neurosci Abstr 16:1219

Fleagle JG (1988) Primate adaptation and evolution. Academic Press, San Diego

Freese CH, Oppenheimer JR (1981) The capuchin monkeys, genus *Cebus*. In: Coimbra-Filho AF, Mittermeier RA (eds) Ecology and behavior of neotropical primates. Academia Brasileira de Ciências, Rio de Janeiro, pp 331–390

Gattass R, Oswaldo-Cruz E, Sousa APB (1978) Visuotopic organization of the *Cebus* pulvinar: a double representation of the contralateral hemifield. Brain Res 152:1–16

Gattass R, Rosa MGP, Sousa APB, Piñon MCGP, Fiorani Jr. M, Neuenschwander S, Moura MM, Abrahão JH, Saraiva PES (1990a) Visual topography and modular organization of cortical areas in primates. In: Iwai E and Mishkin M (eds) Vision, memory and temporal lobe. Elsevier, New York, pp 355–367

Gattass R, Rosa MGP, Sousa APB, Piñon MCGP, Fiorani Jr. M, Neuenschwander S (1990b) Cortical streams of visual information processing in primates. Brazil J Med Biol Res 23:375–393

Gattass R, Sousa APB, Rosa MGP (1987) Visual topography of V1 in the *Cebus* monkey. J Comp Neurol 259:529–548

Hendry SCH, Jones EG, Burstein N (1988) Activity-dependent regulation of tachykinin-like immunoreactivity in neurons of monkey visual cortex. J Neurosci 8:1225–1238

Hess DT, Edwards MA (1987) Anatomical demonstration of ocular segregation in the retinogeniculocortical pathway of the New World capuchin monkey *(Cebus apella)*. J Com Neurol 264:409–420

Hoffstetter R (1982) Les primates Simiiformes (=Anthropoidea): comprehénsion, phylogenie, histoire biogéographique. Annales de Paléontologie 68:241–290

Horton JC (1984) Cytochrome oxidase patches: a new cytoarchitectonic feature of monkey visual cortex. Philos Trans R Soc Lond [Biol] 304:199–253

Horton JC, Hubel DG (1981) Regular patchy distribution of cytochrome oxidase staining in primary visual cortex of macaque monkey. Nature 292:762–764

Hubel DH, Wiesel TN (1977) Functional architecture of macaque monkey visual cortex: Ferrier lecture. Proc R Soc Lond [Biol] 198:1–59

Le Gros Clark WE (1959) The antecedents of man. Edinburgh University Press, Edinburgh

Livingstone MS, Hubel DH (1984) Anatomy and physiology of a color system in the primate visual cortex. J Neurosci 4:309–356

Livingstone MS, Hubel DH (1988) Do the relative mapping densities of the magno- and parvocellular systems vary with eccentricity? J Neurosci 8:4334–4339

Mc Illwain JL (1976) Large receptive fields and spatial transformations in the visual system. Int Rev Physiol 10:223–249

Motter BC, Poggio GF (1982) Spatial invariance of receptive field location in the presence of eye movements of fixation for neurons in monkey striate cortex. Soc Neurosci Abstr 8:707

Rosa MGP, Gattass R, Fiorani Jr. M (1988a) Cytochrome oxidase topography in striate cortex of normal and monocularly enucleated *Cebus* monkeys. Soc Neurosci Abstr 14:1123

Rosa MGP, Gattass R, Fiorani Jr. M (1988b) Complete pattern of ocular dominance stripes in V1 of a New World monkey, *Cebus apella*. Exp Brain Res 72:645–648

Rosa MGP, Sousa APB, Gattass R (1988c) Representation of the visual field in the second visual area in the *Cebus* monkey. J. Comp Neurol 275:326–345

Schein SJ, de Monasterio FM (1987) Mapping of retinal and geniculate neurons onto striate cortex of macaque. J. Neurosci 7:996–1009

Silveira LCL, Picanço-Diniz CW, Sampaio LFS, Oswaldo-Cruz E (1989) Retinal ganglion cell distribution in the *Cebus* monkey: a comparison with the central magnification factors. Vision Res 29:1471–1483

Silverman MS, Tootell RBH (1987) Modified technique for cytochrome oxidase histochemistry: increased staining intensity and compatibility with the 2-deoxyglucose autoradiography. J Neurosci Meth 19:1–10

Tootell RBH, Hamilton SL, Silverman MS (1985) Topography of cytochrome oxidase activity in owl monkey cortex. J Neurosci 5:2786–2800

Tootell RBH, Silverman MS (1985) Two methods for flat-mounting cortical tissue. J Neurosci Methods 15:177–190

Tootell RBH, Hamilton SL, Silverman MS, Switkes E (1988a) Functional anatomy of macaque striate cortex. I. Ocular dominance, binocular interactions and baseline conditions. J Neurosci 8:1500–1530

Tootell RBH, Switkes E, Silverman MS, Hamilton SL (1988b) Functional anatomy of macaque striate cortex. II. Retinotopic organization. J Neurosci 8:1531–1568

Trusk TC, Kaboord WS, Wong-Riley MTT (1990) Effects of monocular enucleation, tetrodotoxin, and lid suture on cytochrome-oxidase reactivity in supragranular puffs of adult macaque striate cortex. Vis Neurosci 4:185–204

T'so DY, Gilbert CD (1988) The organization of chromatic and spatial interactions in the primate striate cortex. J Neurosci 8:1712–1727

Wong-Riley MTT (1979) Changes in the visual system of monocularly sutured or enucleated kittens demonstrable with cytochrome oxidase histochemistry. Brain Res 171:11–28

Wong-Riley MTT, Trusk TC, Tripathi SC, Hoppe DA (1989) Effect of retinal impulse blockage on cytochrome oxidase-rich zones in the macaque striate cortex. II. Quantitative electron-microscopic (EM) analysis of neuropil. Vis Neurosci 2:499–514

Wright PC (1981) The night monkeys, genus *Aotus*. In: Coimbra-Filho AF, Mittermeier RA (eds) Ecology and behavior of neotropical primates. Academia Brasileira de Ciências, Rio de Janeiro

Note added in proof. Recently, Trusk and Wong-Riley (Soc Neurosci Abstr 16:708) also observed, in macaques submitted to unilateral retinal lesions, the increase in cytox reactivity in the interpatches overlying the stripes of the intact eye, as compared with normal tissue.